[32]Walker, J. E., Whan, G. A., and Rothfus, R. R., "Fluid Friction in Noncircular Ducts," *AIChE Journal,* Vol. 3, No. 4, 1957, pp. 484-489.

[33]Wilhelm, R. H., Wroghton, D. M., and Loeffel, W. F., "Flow of Suspensions Through Pipes," *Industrial and Engineering Chemistry,* Vol. 31, No. 5, 1939, pp. 622-629.

[34]Bogue, D. C. and Metzner, A. B., "Velocity Profiles in Turbulent Pipe Flow," *Industrial Engineering Chemistry Fundamentals,* Vol. 2 No. 2, 1963, pp. 143-149.

[35]Caldwell, D. H. and Babbitt, H. E., "Turbulent Flow of Sludges in Pipes," *University of Illinois Engineering Experiment Station Bulletin,* No. 323, Nov. 1940.

[36]Murdoch, R. and Kearsey, H. A., "Pumping Studies on Aqueous Throia Slurries," *Transactions of the Institute of Chemical Engineers,* Vol. 38, 1960, pp. 165-175.

[37]Crowley, P. R. and Kitzes, A. S., "Rheological Behavior of Thorium Oxide Slurries in Laminar Flow," *Industrial and Engineering Chemistry,* Vol. 49, 1957, pp. 888-892.

Engineering Notes

ENGINEERING NOTES are short manuscripts describing new developments or important results of a preliminary nature. These Notes cannot exceed 6 manuscript pages and 3 figures; a page of text may be substituted for a figure and vice versa. After informal review by the editors, they may be published within a few months of the date of receipt. Style requirements are the same as for regular contributions (see inside back cover).

Experimental Investigation of a Low Velocity Electrostatic Current Meter

James R. Williford* and David L. Murphree†
Mississippi State University, State College, Miss.

Introduction

THE present instrumentation state-of-the-art for measuring water movement includes hot film probes, Savonius rotor meters, electromagnetic meters, vortex shedding meters, and acoustic Doppler meters.[1] Whenever the temperature of the water varies between calibration and velocity measurement or during measurements, the influence of temperature on the hot film sensor must be considered. The rotating vane meter and vortex meter are insensitive to extremely low velocities, i.e., less than 0.1 fps. They are also especially inadequate for sensing small perturbations in ocean currents. The size and shape of the electromagnetic meter cause water distortion relative to its normally constant relationship to the freestream velocity, which may result in false measurements. The quality of the reflected signal and calibration difficulties are problems associated with the acoustic Doppler meters.

A need exists for more accurate measurements of the low velocity currents and small perturbations in ocean currents than can be obtained with the previously mentioned meters. These low velocities and small perturbations in the ocean currents have proved to be especially important near the ocean floor. These currents and perturbations have been instrumental to the build up or degradation of the ocean bottom, the migration of microscopic organisms, and the resulting migration of the larger forms of sea life which feed on them.

Electrostatic probes have been utilized successfully to measure the velocity of a flowing ionized gas.[2] This Note describes an experimental investigation of an electrostatic current meter which was found to be very sensitive to low velocities in sea water. The current meter demonstrates sensitivity to water velocities of less than 0.1 fps and small perturbations in the velocity. Although tests were not performed to directly measure the frequency response of the current meter, the meter did appear to exhibit a nearly instantaneous time response.

Received November 19, 1973; revision received October 4, 1974.
Index categories: Oceanography, Physical and Biological.

*Research Engineer, Department of Aerophysics and Aerospace Engineering.
†Professor, Department of Aerophysics and Aerospace Engineering.

Theory of Operation

The investigated electrostatic current meter operates on the principle of electrolysis of sea water superimposed on the mass motion of the water past the meter. Every metal when immersed in an electrolytic solution and subjected to an increasing applied potential will conduct an almost constant current until a certain potential is reached.[3] At this potential, called the decomposition voltage, a sharp increase in the amount of current passed occurs. At the decomposition voltage steady electrolysis commences, and evolution of hydrogen and oxygen bubbles begins. It is above this potential that the current meter must be operated. Once above the decomposition voltage it is the superposition of the mass motion of the medium onto the normal electrolytic process that gives the current meter its sensitivity to the velocity of the sea water.

Obviously the meter is sensitive to the salinity of the water. However this should present no problem in the application of the device since it would be used in situ and the salinity of the site would be known. No investigation was made to determine the effect of temperature and pressure. These parameters will have an effect on the behavior of the meter,[4] however the effect may possibly be negated through the use of compensating methods similar to those used with hot wire anemometers.

Experimental Apparatus

To simulate sea water, a solution consisting of 35 parts of salt to 1000 parts of tap water by weight was used. To create the relative motion of the meter and water, a stationary channel of water with the meter mounted on a cart on a track was employed. The cart was moved along the track by means of a line attached from the cart to a spool attached to a system of gears driven by a low speed d.c. motor. With this system it was possible to measure very accurately the relative velocity between the meter and water by timing the motion between several reference points marked on the track.

The current meter geometry used for this experiment is shown in Fig. 1. It consists of two copper electrodes, one being number 26 wire and the other a flat disk of approximately ½ in. diam. The current meter was most sensitive when the wire was used as the negative electrode. Hence, this was the configuration used in the experiment.

Two different techniques of operating the electrostatic current meter were tested. The first method used was to apply

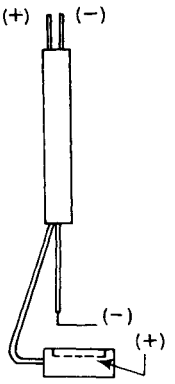

Fig. 1 Electrostatic current meter geometry.

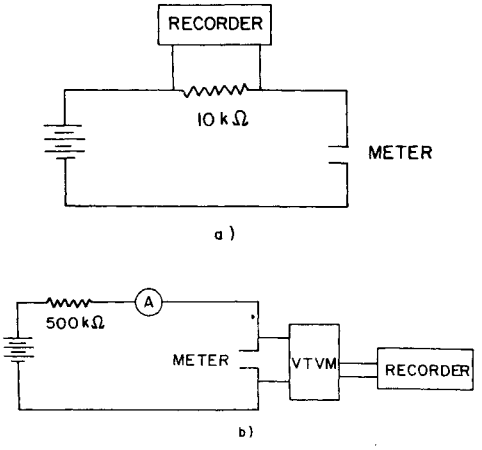

Fig. 2 Schematic for a) constant applied voltage method and b) constant current method.

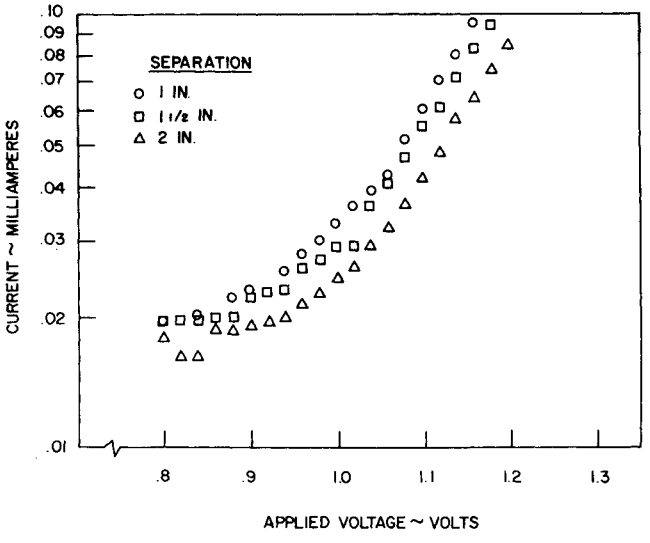

Fig. 3 Decomposition curve for copper.

a constant voltage across the meter with a 10k ohm resistor in series with it. This circuit is shown in Fig. 2a. Changes in water velocity produced corresponding changes in voltage across the resistor, and these voltages were plotted by the recorder.

The second method of operation was to maintain a constant current through the meter and record the voltage change of the meter with corresponding changes in water velocity. The circuit used for this technique is shown in Fig. 2b. Constant

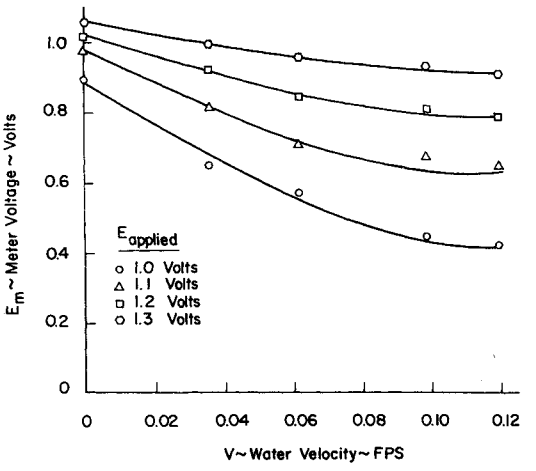

Fig. 4 Meter voltage vs velocity for constant applied voltage.

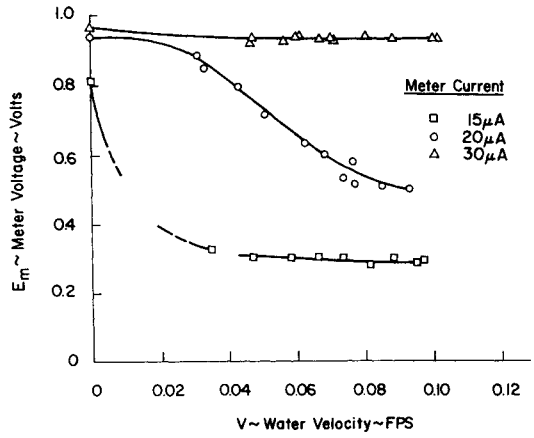

Fig. 5 Meter voltage vs velocity for constant current.

current through the meter was achieved by setting the supply voltage at approximately 30v. The 500k ohm resistor then made the total circuit impedance appear constant, hence the current remained constant.

Experiment and Results

The decomposition voltage of the copper electrodes used for the current meter and the effect of the separation distance between the anode and cathode on the overall decomposition curve were determined by mounting the electrodes in a tank at various separation distances. The result of this investigation is shown in Fig. 3. The decomposition curve of the electrodes is essentially independent of the distance between them. Hence no restriction is made in constructing the meter as far as the distance between the electrodes is concerned.

The results of operating the current meter at a constant applied voltage are shown in Fig. 4. These curves were generated by conducting several tests at different applied potentials. The current meter sensitivity to the velocity increases as applied voltage decreases. The sensitivity of the meter to velocities in the 0 to 0.1 fps range is also revealed in Fig. 4.

Operating the current meter at constant electrical current generated the curves shown in Fig. 5. For 15 μa passing through the current meter, it is sensitive to velocities of less than 0.01 fps. At 20 μa of current passing through the current meter, it demonstrated sensitivities throughout the range of velocities tested.

As electrolysis proceeded on the electrodes, there occurred no measurable change in the meter's sensitivity. Tests were made to determine if the meter was sensitive to direction by

aligning the meter at different angles to the flow direction. A noticeable directional sensitivity was not detected since no change in output characteristics were observed.

Conclusion

Disassociated sodium chloride in sea water provides positive and negative charge carriers which can be utilized for measurement of low velocities in the ocean. The electrostatic current meter demonstrated a remarkable sensitivity to the velocity in sea water due to the effect of the mass motion of the medium superimposed on the normal migration of charged particles under the influence of the electrostatic potential.

References

[1]Appell, G. F. and Woodward, W. E., "Review of Current Meter Technology," *Under Sea Technology*, Vol. 14, No. 6, June 1973, pp. 16-18.

[2]Johnson, B. H. and Murphree, D. L., "Plasma Velocity Determination by Electrostatic Probes," *AIAA Journal*, Vol. 7, No. 10, Oct. 1969, pp. 2028-2030.

[3]Glasstone, S., *Elements of Physical Chemistry*, Van Nostrand, Princeton, N.J., 1960, pp. 492-504.

[4]Holmes, J. F., "Wide Range Flow Meter for Oceanographic Measurements," *Proceedings of the Marine Sciences Symposium*, Miami, Fla., 1965, pp. 251-255.

Turning Moment on a Rotating Disk

J. Richard Shanebrook*
Union College, Schenectady, N. Y.
and
David McMullan†
General Electric Company, Schenectady, N. Y.

Nomenclature

C_M = $2M/\frac{1}{2}\rho\omega^2 r_o^5$, the dimensionless moment coefficient
M = turning moment on one side of the disk
r = radial distance measured from the axis of rotation of the disk
r_c = radius at which transition occurs
r_o = radius of the disk
R = $r_o^2\omega/\upsilon$, the Reynolds number based on r_o and the tip velocity.
R_c = $r_c^2\omega/\upsilon$, the critical Reynolds number.
υ = kinematic viscosity of the fluid
ω = uniform angular velocity of the disk
ρ = density of the fluid

Subscripts

l = laminar flow
t = turbulent flow

EXPERIMENTAL results, such as those given by Gregory, Stuart, and Walker,[1] indicate that the flowfield on a rotating disk consists of three distinct flow regimes in the most general case where transition to turbulence has occurred in the boundary layer. That is, there is a laminar flow region surrounding the axis of rotation which is followed by a transitional region and then a fully turbulent region which extends to the tip of the disk. The situation is somewhat analogous to the flowfield on a flat plate which has a laminar leading edge region followed by transitional and fully turbulent regions. The purpose here is to develop an equation for the turning moment on a rotating disk that accounts for the extent of the laminar and turbulent flow regions. The approach is similar to that used to determine the drag on a flat plate when both laminar and turbulent flow regions are present (e.g., see Schlichting,[2] pp. 600-601).

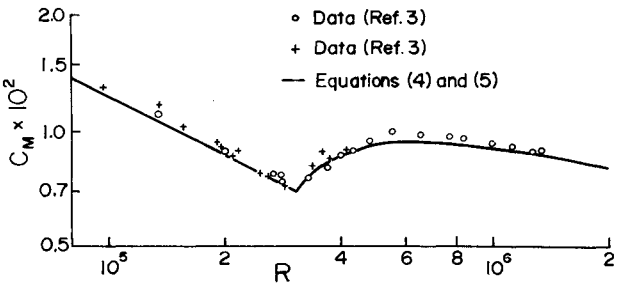

Fig. 1 Experimental data from Ref. 3 compared with Eqs. (4) and (5). Equation (4) is shown for $R>3.1\text{x}10^5$, and Eq. (5) is shown for smaller Reynolds numbers.

According to Schlichting,[2] the turning moment on one side of a disk of radius, r_o, with a wholly laminar flowfield on its surface is

$$M_l = \tfrac{1}{4}(3.87)\rho\omega^2 r_o^5 (r_o^5\omega/\upsilon)^{-1/2} \tag{1}$$

For the case of a wholly turbulent flowfield the turning moment can be evaluated from the von Karman relation[2]

$$M_t = \tfrac{1}{4}(0.146)\rho\omega^2 r_o^5 (r_o^2\omega/\upsilon)^{-1/5} \tag{2}$$

In the latter case, the initial laminar flow region can be simply accounted for if it is assumed that after transition the boundary layer behaves as if it were turbulent from the axis of rotation of the disk. That is, the turning moment on the disk is then found by subtracting from Eq. (2) the amount of turbulent torque acting on the disk from the axis of rotation to the circle of transition and then adding the laminar torque for the same circular region. Thus the turning moment on one side of the disk, accounting for the laminar and turbulent flow regions, is

$$M = \tfrac{1}{4}(0.146)\rho\omega^2 r_o^5 (r_o^2\omega/\upsilon)^{-1/5} - \tfrac{1}{4}(0.146)\rho\omega^2 r_c^5 (r_c^2\omega/\upsilon)^{-1/5} + \tfrac{1}{4}(3.87)\rho\omega^2 r_c^5 (r_c^2\omega/\upsilon)^{-1/2} \tag{3}$$

where r_c denotes the radius at which transition occurs. Introducing the critical Reynolds number, Eq. (3) can be arranged in the form

$$C_M = 3.87\,R^{-5/2}R_c^2 + 0.146\,R^{-1/5}\,[1-(R_c/R)^{2.3}\,] \tag{4}$$

where C_M is the dimensionless moment coefficient defined in the Nomenclature.

Figure 1 compares the experimental values of dimensionless moment coefficient reported by Theodorsen and Regier[3] with the values computed from Eq. (4) assuming a critical Reynolds number of $3.1\text{x}10^5$. It is seen that the theory is in good agreement with the experimental results. Finally, it is noted that Eq. (4) is valid only for Reynolds numbers R that are greater than the critical Reynolds number (thus, Eq. (4) is shown in Fig. 1 only for $R>3.1\text{x}10^5$). For smaller Reynolds numbers, the flow is wholly laminar and Eq. (1) must be used

Received June 10, 1974.
Index category: Hydrodynamics.

*Associate Professor, Department of Mechanical Engineering. Member AIAA.

†Engineer, Thermal Design and Performance Analysis, S8G Project, Knolls Atomic Power Laboratory.

for the computation of turning moments. Written in dimensionless form, Eq. (1) becomes

$$C_M = 3.87\,R^{-1/2} \tag{5}$$

which, for the sake of completeness, is also shown in Fig. 1 for $R \leq 3.1 \times 10^5$.

References

[1]Gregory, N., Stuart, J. T., and Walker, W. S., "On the Stability of Three-Dimensional Boundary Layers with Application to the Flow Due to a Rotating Disk," *Royal Society of London, Philosophical Transactions*, Vol. A 248, July 1955, pp. 155-199.

[2]Schlichting, H., *Boundary-Layer Theory*, McGraw-Hill, New York, 1968.

[3]Theodorsen, T. and Regier, A., "Experiments on Drag of Revolving Disks, Cylinders, and Streamline Rods at High Speeds," Rept. 793, 1944, NACA.

Velocity Distribution Equation for Laminar Unidirectional Flow in an Equilateral Triangular Conduit

R. Elangovan*
Process Research Inc., Cincinnati, Ohio

Introduction

A SIMPLE closed form solution to the Navier-Stokes equation for the laminar flow in an equilateral triangular conduit of side a is presented by Landau and Lifshitz.[1] This solution is of the form

$$u(x,y) = -\frac{2}{3^{1/2} a u}\left(\frac{dp}{dz}\right) h_1\, h_2\, h_3 \tag{1}$$

where h_1, h_2, h_3 are the lengths of the perpendiculars from a given point in the triangle to its three sides, dp/dz is the constant pressure gradient, and a the length of each side of the triangle (Fig. 1). This Note shows that Eq. (1) results as a first approximation to more accurate and general variational solution of the Navier-Stokes equation. Variational solutions to the Navier-Stokes equation for other triangular geometries and rectangular geometries can also be obtained.

Variational Solution

For the coordinate system shown in Fig. 1, the Navier-Stokes equation can be written as

$$\left(\frac{\partial^2 u}{\partial x^2}\right) + \left(\frac{\partial^2 u}{\partial y^2}\right) = \frac{1}{\mu}\frac{dp}{dz} \tag{2}$$

The functional for the Navier-Stokes Equation (2) and for the geometry shown in Fig. 1 can be written as

$$I(u) = \int_{x=0}^{x=3^{1/2}a/2} \int_{y=-x/3^{1/2}}^{y=+x/3^{1/2}} \left[\left(\frac{\partial u}{\partial x}\right)^2 + \left(\frac{\partial u}{\partial y}\right)^2 + 2u\left(\frac{1}{\mu}\frac{dp}{dz}\right)\right] dx\,dy \tag{3}$$

$$u(x,y) = 0 \qquad \text{on the boundary} \tag{4}$$

If the function $u(x,y)$ gives a minimum for the integral Eq. (3) it must satisfy Eq. (2).

Following the Kontorovich[2] variational method, we choose a sequence of coordinate system of functions $f_1(x,y)$, $f_2(x,y)$, ..., $f_n(x,y)$ and seek the solution of the variational problem in the form of a sum of the functions

$$u_n = \sum_{k=1}^{n} v_k(x)\, f_k(x,y) \tag{5}$$

where the coefficients $v_k(x)$ are not constants but are unknown functions of one of the independent variables that we define so that the functional $I(u)$ is extremized.

The first approximation to Eq. (5) is given by

$$u_1 = [y^2 - (x/3^{1/2})^2]\, v_1(x) \tag{6}$$

where

$$[y^2 - (x/3^{1/2})^2] = f_1(x,y)$$

The boundary condition Eq. (4), on the straight lines (Fig. 1) $y = \pm x/3^{1/2}$ are satisfied by u_1 for such a choice of $f_1(x,y)$. With this choice of u_1 Eq. (3) becomes after integration

$$I(u_1) = \frac{8 \times 3^{1/2}}{405} \int_{x=0}^{x=3^{1/2}a/2} [2x^5 (v_1')^2 + 10x^4 v_1 v_1' + 30x^3 v_1^2 - 15\left(\frac{1}{\mu}\frac{dp}{dz}\right) x^3 v_1]\,dx = \int_{x_0}^{x_1} F[x,\, v_1(x),\, v_1'(x)]\,dx \tag{7}$$

The function $v_1(x)$ is chosen so that the functional $I(u_1)$ is extremized. Hence $v_1(x)$ must satisfy Euler's equation

$$F_{v_1} - \frac{d}{dx}(F_{v_1'}) = 0 \tag{8}$$

i.e.,

$$x^2 v_1'' + 5x\, v_1' - 5v_1 = -\left(\frac{15}{4}\right)\left(\frac{1}{\mu}\right)\left(\frac{dp}{dz}\right) \tag{9}$$

The solution of Eq. (9) is

$$v_1(x) = Ax + Bx^{-5} + \frac{3}{4}\left(\frac{1}{\mu}\frac{dp}{dz}\right) \tag{10}$$

At $x = 0$, $v_1(x)$ must be finite

$$\text{At } x = \frac{3^{1/2}}{2}a,\ v_1(x) = 0 \tag{11}$$

Therefore,

$$v_1(x) = \frac{3^{1/2}}{2a}\left(\frac{1}{\mu}\frac{dp}{dz}\right)\left(\frac{3^{1/2}a}{2} - x\right) \tag{12}$$

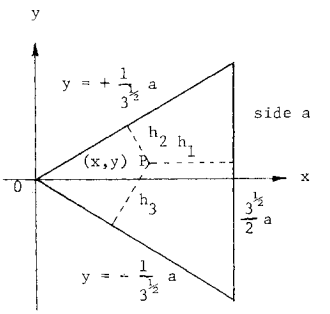

Fig. 1 Coordinates for an equilateral triangular cross section.

Received September 30, 1974.
Index category: Nozzle and Channel Flow.
*Mechanical Engineer.